

Sm(III) Complexation with amino acids. Crystal structures of $[\text{Sm}_2(\text{Pro})_6(\text{H}_2\text{O})_6](\text{ClO}_4)_6$ and $[\text{Sm}(\text{Asp})(\text{H}_2\text{O})_4]\text{Cl}_2$

Julia Torres,^a Carlos Kremer,^{*a} Eduardo Kremer,^a Helena Pardo,^b Leopoldo Suescun,^b Álvaro Mombrú,^b Sixto Domínguez,^c Alfredo Mederos,^c Regine Herbst-Irmer^d and Juan M. Arrieta^e

^a Cátedra de Química Inorgánica, Facultad de Química, CC1157, Montevideo, Uruguay. E-mail: ckremer@bilbo.edu.uy

^b Laboratorio de Cristalografía, Facultad de Química, CC1157, Montevideo, Uruguay

^c Departamento de Química Inorgánica, Universidad de La Laguna, Tenerife, Canary Islands, Spain

^d Department of Structural Chemistry, Inorganic Chemistry Institute, D-37077, Göttingen, Germany

^e Departamento de Química Inorgánica, Universidad del País Vasco-E.H.U., Bilbao, Spain

Received 29th April 2002, Accepted 5th August 2002

First published as an Advance Article on the web 8th October 2002

Samarium complexes with amino acids have been studied by potentiometric measurements. Experiments were performed in aqueous solution at 37.0 °C and 0.15 M NaClO₄, resembling physiological medium. Low stability Sm(III)–amino acid complexes were detected. Complexes with 1 : 1 ligand to metal molar ratios are predominant in the studied pH interval. Other mono- and di-nuclear species can be detected up to pH 6. For higher pH values, hydrolysis to $[\text{Sm}(\text{OH})]^{2+}$ and $\text{Sm}(\text{OH})_3$ becomes the main process. Some of the studied complexes were isolated and characterized in the solid state. Single-crystal X-ray structures of $[\text{Sm}_2(\text{Pro})_6(\text{H}_2\text{O})_6](\text{ClO}_4)_6$ (**1**) and $[\text{Sm}(\text{Asp})(\text{H}_2\text{O})_4]\text{Cl}_2$ (**2**) are reported. In both complexes, an eight coordinate Sm atom is found, surrounded by carboxylate groups and water molecules. In **1**, Sm atoms form infinite chains bridged by proline ligands (via carboxylate groups). An additional monodentate amino acid is present in the coordination sphere of each Sm center. In **2**, the amino acid also bridges Sm atoms but using α and β carboxylate groups. The overall structure consists of infinite planes in which all carboxylate groups, acting as bidentate ligands, are bonded to Sm atoms.

Introduction

¹⁵³Sm coordination compounds are successfully used as radiotherapeutic agents due to the excellent nuclear properties of this nuclide. ¹⁵³Sm (β^- emitter) has a half life (46.27 h) short enough to deliver an appropriate dose of radiation in a relatively brief period. Besides, this radionuclide emits gamma rays that are nearly ideal for planar or SPECT scintigraphic imaging. This allows to follow the distribution of the radionuclide *in vivo* and to estimate absorbed doses in patients.^{1–3} For example, complexes of samarium(III) with phosphonate chelating agents such as ¹⁵³Sm-EDTMP (EDTMP = ethylenediamine-tetramethylene-phosphonic acid) have already been used to treat skeletal metastases.⁴ These facts have promoted the development of the basic coordination chemistry of this 4f transition element.

A crucial point in designing new radiotherapeutic agents is to obtain stable complexes which are able to reach tumor cells. Amino acids (H_nL in their zwitterionic form) participate in the transportation of metal ions in living organisms, forming metal–amino acid complexes. Then, Sm(III)–amino acid complexes could be suitable for transporting this nuclide to its target. On the other hand, amino acid intake (as well as for some other small molecules) by abnormal cells is enhanced due to the special metabolism of such cells. So, it is possible to hypothesize that the intake of Sm(III) complexes with these ligands would be preferential for abnormal tissues. As a consequence, coordinating amino acids to Sm(III) looks a promising way to search for new radiotherapeutic agents of this nuclide.

In a previous paper we reported on the study of Sm(III) complexation with glycine (Gly), alanine (Ala), valine (Val),

cysteine (Cys), proline (Pro), tryptophan (Trp) and glutamic acid (Glu) under physiological conditions.⁵ Even when mono- and di-nuclear species can be detected, they are not stable enough to compete with the formation of $\text{Sm}(\text{OH})_3$ (s) at pH 7.0. However, results depend on the particular amino acid.

As a continuation of this work and searching for stable complexes, stability studies on samarium coordination compounds with other α -amino acids and one β -amino acid have been carried out. Sm(III) complexation with arginine (Arg), serine (Ser), phenylalanine (Phe), aspartic acid (Asp), histidine (His) and β -alanine (β -Ala) is here reported.

Experimental conditions have been chosen to resemble physiological medium (37.0 °C, NaClO₄ 0.15 M) and the obtained results have been corrected, taking into account the hydrolysis reactions of samarium(III), *i.e.* the formation of $[\text{Sm}(\text{OH})]^{2+}$ and $\text{Sm}(\text{OH})_3$ (s) in that medium.⁶

In order to explore the structure of these complexes in depth, some of them were prepared and isolated in the solid state. $[\text{Sm}_2(\text{Pro})_6(\text{H}_2\text{O})_6](\text{ClO}_4)_6$ and $[\text{Sm}(\text{Asp})(\text{H}_2\text{O})_4]\text{Cl}_2$ were fully characterized by X-ray diffraction techniques.

Experimental

Materials and equipment

All common laboratory chemicals were reagent grade, purchased from commercial sources and used without further purification. All solutions were freed of carbon dioxide by Ar bubbling. The standard HCl and NaOH solutions were prepared from Merck standard ampoules. Sm(III) stock solutions

were prepared using $\text{SmCl}_3 \cdot 6\text{H}_2\text{O}$ from Aldrich and standardized volumetrically by titration with sodium ethylenediaminetetraacetate ($\text{Na}_2\text{H}_2\text{edta}$ from Sigma) at constant pH 5.0, in the presence of sodium methyl thymol blue as visual indicator.

Infrared spectra were recorded on a Bomem FT-IR spectrophotometer as 1% KBr pellets. Elemental analyses were performed on a Carlo Erba EA1108. Thermal analyses were performed on a Shimadzu Dta-50, TGA-50 with TA50I interface, using a platinum cell and nitrogen atmosphere (this equipment was a gift from the Japanese Government). The experimental conditions were the following: temperature ramp rate, 5°C min^{-1} up to 200°C held for 10 min; nitrogen flow rate, 50 mL min^{-1} .

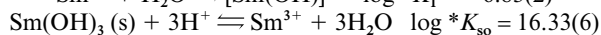
Potentiometric measurements

At least two potentiometric titrations (*ca.* 150 experimental points each) were performed for the determination of the protonation constants of amino acids, in the concentration interval 10–20 mM, covering pH values between 2.0 and 11.0.

At least three potentiometric titrations (*ca.* 100 experimental points each) of acid stock solutions of SmCl_3 (concentrations ranging from *ca.* 5.0 to 10.0 mM) were carried out in the presence of the ligands, using different ligand to metal molar ratios (1 : 1 to 5 : 1). The samarium concentration interval was chosen taking into account the existing data, the experimental errors and the fact that for radiotherapeutic purposes, low metal concentrations are used (*ca.* 3 mM). pH values between 2.0 and the precipitation of $\text{Sm}(\text{OH})_3$ (s) were covered.

These solutions were poured into a 50 mL titration cell and, after thermal equilibrium was reached, the hydrogen ion concentration was determined by a number of successive readings after each addition of small increments of standard 0.1 M NaOH solution. The e.m.f. were recorded by a Metrohm 713 pH Meter, using a glass electrode and a Ag/AgCl reference electrode. The ionic strength was kept constant throughout the titrations by using solutions containing 0.15 M NaClO_4 and a relatively low concentration of metal ion. Pre-saturated argon (free of CO_2) was bubbled through the solutions during the titrations to eliminate the adverse effect of atmospheric carbon dioxide, and the temperature was kept at $37.0 \pm 0.1^\circ\text{C}$. The cell constants E° and the liquid junction potentials were determined according to the methods of Sillén⁷ and Liberti and Light.⁸ Data were analyzed using the HYPERQUAD program,⁹ and distribution species diagrams were produced using the HySS program.¹⁰

In order to study these $\text{Sm}(\text{III})\text{--H}_n\text{L}$ systems, previous hydrolysis studies (under identical conditions)⁶ were taken into account, in particular the formation of $[\text{Sm}(\text{OH})]^{2+}$ and $\text{Sm}(\text{OH})_3$ (s):



Synthesis

[Sm₂(Pro)₆(H₂O)₆](ClO₄)₆ 1. Pro (32 mg, 0.28 mmol), $\text{SmCl}_3 \cdot 6\text{H}_2\text{O}$ (100 mg, 0.27 mmol) and $\text{NaClO}_4 \cdot \text{H}_2\text{O}$ (77 mg, 0.55 mmol) were dissolved in 2 mL water. The pH was adjusted to 4.4 and the resulting solution was allowed to evaporate at room temperature. Slow evaporation (and after white crystals of sodium perchlorate were separated) afforded pale yellow crystals of **1** (40 mg, 45%). A prismatic crystal suitable for X-ray diffraction was also collected. (Found: C, 20.3; H, 3.7; N, 4.7. $\text{Sm}_2\text{C}_{30}\text{H}_{66}\text{O}_{42}\text{N}_6\text{Cl}_6$ requires C, 21.2; H, 3.9; N, 5.0%). TGA analysis agreed with the proposed formula (6.1% loss of weight corresponding to the elimination of water, calculated 6.4%). $\nu_{\text{max}}/\text{cm}^{-1}$ (NH_2) 3448s, (CO) 1602s, 1438m, (ClO_4^-) 1145vs, 1116vs, 1087vs.

Table 1 Crystal data and structural refinement parameters for structures **1** and **2**

	1	2
Chemical formula	$\text{SmC}_{15}\text{H}_{33}\text{O}_{21}\text{N}_3\text{Cl}_3$	$\text{SmC}_4\text{H}_{14}\text{O}_8\text{NCl}_2$
<i>M</i>	848.18	425.41
Space group	$P\bar{1}$	$P2_1$
<i>a</i> /Å	13.052(4)	9.1372(18)
<i>b</i> /Å	13.725(3)	7.6379(15)
<i>c</i> /Å	9.929(3)	9.2014(18)
$\alpha/^\circ$	110.34(2)	90
$\beta/^\circ$	100.73(2)	91.57(3)
$\gamma/^\circ$	109.62(2)	90
<i>V</i> /Å ³	1475.6(7)	641.9(2)
<i>Z</i>	2	2
μ/mm^{-1}	2.354	5.013
<i>F</i> (000)	838	410
Crystal dimensions /mm	$0.1 \times 0.1 \times 0.2$	$0.25 \times 0.14 \times 0.08$
Reflections collected	7942	4919
Independent reflections	6071	2413
[<i>I</i> > 2σ <i>I</i>]		
<i>R</i> 1 ^a	0.0489	0.0353
<i>wR</i> 2 ^b	0.1353	0.0887

$$^a R1 = \sum |F_o| - |F_c| / \sum |F_o|, \quad ^b wR2 = \{ \sum [w(F_o^2 - F_c^2)^2] / \sum [w(F_o^2)^2] \}^{1/2}$$

[Sm(Asp)(H₂O)₄]Cl₂ 2. Asp (180 mg, 1.35 mmol) was dissolved in 8 mL of 1 M hydrochloric acid solution. Then, $\text{SmCl}_3 \cdot 6\text{H}_2\text{O}$ (500 mg, 1.37 mmol) was added. The pH was adjusted to 2.6 with 1 M LiOH and the resulting solution was allowed to evaporate at room temperature. Slow evaporation afforded pale yellow crystals of **2** (86 mg, 15%). Some of them were suitable for X-ray diffraction. (Found: C, 11.2; H, 3.3; N, 3.3. $\text{SmC}_4\text{H}_{14}\text{O}_8\text{NCl}_2$ requires C, 11.3; H, 3.3; N, 3.3%). TGA analysis agreed with the proposed formula (18.8% loss of weight corresponding to the elimination of water, calculated 16.9%). $\nu_{\text{max}}/\text{cm}^{-1}$ (NH_2) 3401s, (CO) 1624s, 1437m.

X-Ray data collection and structure solution

X-Ray data collection for **1** was performed at room temperature [298(2) K] on a Rigaku AFC-7S diffractometer¹¹ using monochromated (graphite) Mo-*K* α radiation ($\lambda = 0.7107 \text{ \AA}$) in the ω - 2θ scan mode. During the data collection the intensity of three standard reflections was monitored every 150 measurements to correct for intensity decay. Lorentz, polarization and absorption corrections were applied. Data collection for **2** was performed at room temperature [293(2) K] with a STOE IPDS (STOE, 1988) X-ray diffractometer. Absorption correction was performed by ϕ -scans¹² and extinction correction was applied. Relevant crystallographic data are shown in Table 1.

The structures of both compounds were solved by direct methods locating most non-hydrogen atoms. It was completed by successive difference Fourier maps. In **1**, refinement was anisotropic for all non-hydrogen atoms except for two oxygen atoms belonging to one of the four perchlorates present in this structure. Refinement was anisotropic for all non-hydrogen atoms in **2**.

All hydrogen atoms were calculated at idealized positions and with fixed distances [0.98 Å for $\text{C}_{(\text{tertiary})}\text{--H}$, 0.97 Å for $\text{C}_{(\text{secondary})}\text{--H}$, and 0.90 Å for $\text{N}_{(\text{Pro})}\text{--H}$ in **1**, and 0.98 Å for $\text{C}_{(\text{tertiary})}\text{--H}$, 0.97 Å for $\text{C}_{(\text{secondary})}\text{--H}$, and 0.89 Å for $\text{N}_{(\text{Asp})}\text{--H}$ in **2**] and refined with isotropic displacement parameters related to the equivalent isotropic displacement parameter of the atom to which it is bonded. The hydrogen atoms from the water molecules attached to samarium were neither found nor calculated in **1**, while in **2** they were located and refined with several restraints and a common isotropic temperature factor. Both structure determinations were achieved using SHELXS¹² and refinement was done using SHELXL programs included in the SHELX-97¹³ package. Geometric calculations and structural

Table 2 Protonation constants of amino acids at 37.0 °C and $I = 0.15$ M NaClO₄

	σ	$\log \beta_{11}$	$\log \beta_{12}$	$\log \beta_{13}$
Ser	0.9	8.773(2)	10.931(6)	
Arg	1.1	8.714(2)	10.641(3)	
His	1.1	8.760(5)	14.61(1)	16.22(3)
Phe	0.9	8.771(6)	10.96(2)	
Asp	1.2	9.230(4)	12.844(8)	14.72(1)
β -Ala	2.4	9.709(5)	13.255(9)	

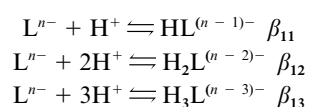
checking were performed with the PLATON-98 program.¹⁴ The ZORTEP program¹⁵ was used to plot the drawings.

CCDC reference numbers 184683 (for **1**) and 184684 (for **2**).

See <http://www.rsc.org/suppdata/dt/b2/b204095f/> for crystallographic data in CIF or other electronic format.

Results and discussion

The protonation constants found for the studied amino acids (H_nL) are depicted in Table 2. H_nL represents the zwitterionic form of amino acids ($n = 1$ for Ser, Arg, His, Phe and β -Ala, $n = 2$ for Asp). The corresponding processes are:



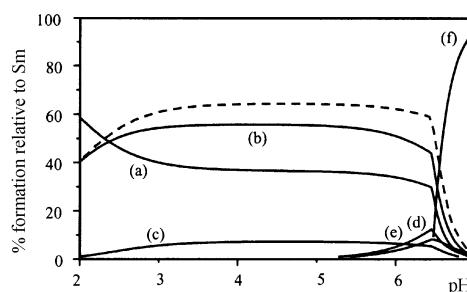
The obtained results for the studied amino acids are in line with those previously reported (if available in similar conditions).^{16–22}

The formation of Sm(III) complexes with amino acids in aqueous solution is only possible at those pH values in which $Sm(OH)_3$ (s) formation does not compete. Beyond pH 6, the precipitation of the hydroxide is a serious competitive product. Even when formation constants have been reported in various aqueous media,^{23–25} they do not include hydrolysis reactions (see Experimental section). The obtained potentiometric results, together with the experimental conditions, are depicted in Table 3. These results are in line with those previously reported for other amino acids.⁵ Not very stable samarium complexes with amino acids are detected in the acid region. They generally give place to deprotonated species and finally to samarium hydroxide when the pH is raised.

Table 3 Stability constants of Sm(III) complexes with amino acids at 37.0 °C and $I = 0.15$ M NaClO₄

	Equilibria	σ	$\log \beta$
Ser	$Sm^{3+} + L^- + H^+ \rightleftharpoons [Sm(HL)]^{3+}$	2.4	11.05(3)
	$Sm^{3+} + L^- \rightleftharpoons [Sm(HL)(OH)_2]^{2+} + H^+$		-3.7(1)
	$Sm^{3+} + 3L^- + 3H^+ \rightleftharpoons [Sm(HL)_3]^{3+}$		31.72(8)
	$Sm^{3+} + 3L^- + 2H^+ \rightleftharpoons [Sm(HL)_3(OH)]^{2+}$		25.65(5)
Arg	$Sm^{3+} + L^- + H^+ \rightleftharpoons [Sm(HL)]^{3+}$	1.3	9.84(5)
	$Sm^{3+} + L^- \rightleftharpoons [Sm(HL)(OH)]^{2+}$		5.91(2)
His	$Sm^{3+} + L^- + 2H^+ \rightleftharpoons [Sm(H_2L)]^{4+}$	1.6	17.43(3)
	$Sm^{3+} + L^- + H^+ \rightleftharpoons [Sm(HL)]^{3+}$		11.63(3)
	$2Sm^{3+} + 4L^- + 6H^+ \rightleftharpoons [Sm_2(HL)_2(H_2L)_2]^{8+}$		59.25(6)
	$Sm^{3+} + 3L^- + 3H^+ \rightleftharpoons [Sm(HL)_3]^{3+}$		33.42(4)
Phe	$Sm^{3+} + L^- + H^+ \rightleftharpoons [Sm(HL)]^{3+}$	2.0	11.49(4)
	$Sm^{3+} + 2L^- \rightleftharpoons [Sm(HL)_2(OH)]^{2+}$		7.95(9)
Asp	$Sm^{3+} + L^{2-} + 2H^+ \rightleftharpoons [Sm(H_2L)]^{3+}$	1.4	14.89(8)
	$Sm^{3+} + L^{2-} + H^+ \rightleftharpoons [Sm(HL)]^{2+}$		11.84(5)
	$Sm^{3+} + L^{2-} \rightleftharpoons [Sm(HL)(OH)]^+$		5.56(5)
	$Sm^{3+} + L^{2-} \rightleftharpoons [Sm(HL)(OH)_2] + H^+$		-1.80(5)
β -Ala	$Sm^{3+} + L^- + H^+ \rightleftharpoons [Sm(HL)]^{3+}$	1.9	11.71(3)
	$Sm^{3+} + L^- \rightleftharpoons [Sm(HL)(OH)_2]^{2+} + H^+$		-1.83(3)

In the Sm(III)–serine system, the predominant species are $[Sm(HL)]^{3+}$ and $[Sm(HL)_3]^{3+}$. The species $[Sm(HL)_2]^{3+}$ was not detected probably due to its low proportion, since it is a transition species. $[Sm(HL)]^{3+}$ and $[Sm(HL)_3]^{3+}$ account for a high percentage of metal complexation (more than 60% for $[Sm^{3+}] = 3$ mM, $[Ser] = 9$ mM) from pH 3.0 to 6.1. They disappear afterwards while the hydroxylated complex $[Sm(HL)_3(OH)]^{2+}$ appears, together with a very small proportion of $[Sm(HL)(OH)_2]^+$. Since free amino acid is in its zwitterionic form (HL) in this pH interval, deprotonation of coordinated water molecules is assumed. Beyond pH 6.4, samarium(III) hydroxide appears. Consequently, a percentage of samarium as low as 4% (for $[Sm^{3+}] = 3$ mM, $[Ser] = 9$ mM) is complexed at neutral pH. A distribution species diagram of this system is depicted in Fig. 1. It also shows the variation of samarium complexation vs. pH under the same conditions.

**Fig. 1** Species distribution diagram (37.0 °C, 0.15 M NaClO₄) for the Sm–Ser system. Ligand : metal ratio 3 : 1 and $C_M = 3.0$ mM. Thick lines: % formation of (a) Sm^{3+} , (b) $[Sm(HL)]^{3+}$, (c) $[Sm(HL)_3]^{3+}$, (d) $[Sm(HL)_3(OH)]^{2+}$, (e) $[Sm(OH)_2]^{2+}$, (f) $Sm(OH)_3$ (s). Broken line: % complexed Sm vs. pH under the same conditions.

With Arg, two complexes are formed: $[Sm(HL)]^{3+}$ and $[Sm(HL)(OH)]^{2+}$. The latter is responsible for samarium complexation at nearly neutral pH (up to 32% for $[Sm^{3+}] = 3$ mM, $[Arg] = 9$ mM) at pH 6.9. The precipitation of samarium hydroxide is not observed until pH 6.9, and even at pH 7, under the same conditions, this complex retains 22% of the metal.

$[Sm(Asp)]^{3+}$ had been previously reported²³ (though its formation constant greatly differs from our results). It had been stated that polynuclear species of lanthanides with aspartic acid exist,²⁶ but these kind of complexes were not detected in the present work. The anionic form of this ligand becomes more

significant (as previously reported for Glu) due to the presence of an additional carboxylate group, which possesses a more acidic proton, as can be seen in Table 2. At pH 3, where both H_2L and HL^- have appreciable concentrations, the formation of $[\text{Sm}(\text{H}_2\text{L})]^{3+}$ is detected. Above pH 4, the predominant form of the ligand is HL^- and the complex $[\text{Sm}(\text{HL})]^{2+}$ is formed. This 1 : 1 species is predominant in the pH interval 4–6. Then, around pH 5.5, two hydroxylated species are detected: $[\text{Sm}(\text{HL})(\text{OH})]^+$ and $[\text{Sm}(\text{HL})(\text{OH})_2]$. Despite the low formation constant of these species, they are very important because they prevent the formation of samarium hydroxide up to pH 6.6. At this point, 80% of the metal is still bound to the ligand (for $[\text{Sm}^{3+}] = 3 \text{ mM}$, $[\text{Asp}] = 9 \text{ mM}$). A distribution species diagram of this system is depicted in Fig. 2, together with the variation of samarium complexation vs. pH under the same conditions.

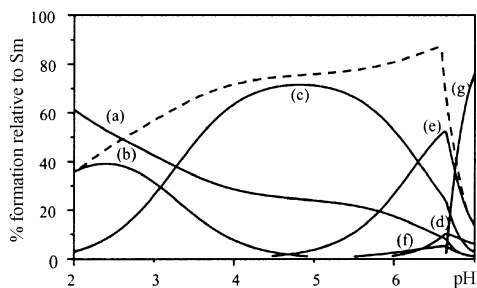


Fig. 2 Species distribution diagram (37.0 °C, 0.15 M NaClO_4) for the Sm–Asp system. Ligand : metal ratio 3 : 1 and $C_M = 3.0 \text{ mM}$. Thick lines: % formation of (a) Sm^{3+} , (b) $[\text{Sm}(\text{H}_2\text{L})]^{3+}$, (c) $[\text{Sm}(\text{HL})]^{2+}$, (d) $[\text{Sm}(\text{HL})(\text{OH})]^+$, (e) $[\text{Sm}(\text{HL})(\text{OH})_2]$, (f) $[\text{Sm}(\text{OH})]^{2+}$, (g) $\text{Sm}(\text{OH})_3 (\text{s})$. Broken line: % complexed Sm vs. pH under the same conditions.

The predominant species in the Sm(III)–Phe system is $[\text{Sm}(\text{HL})]^{3+}$. In the pH 3 to 5 interval (for $[\text{Sm}^{3+}] = 3 \text{ mM}$ and $[\text{Phe}] = 9 \text{ mM}$), it represents more than 70% of the total amount of samarium. Appreciable amounts of $\text{Sm}(\text{OH})_3 (\text{s})$ are formed over pH 6.5

A special comment should be reserved for histidine. In this case, when $[\text{Sm}^{3+}] = 3 \text{ mM}$ and $[\text{His}] = 9 \text{ mM}$, more than 80% of Sm(III) is coordinated, taking into account all complex species, over the pH interval 2.5 to 6.7. This amino acid shows higher coordinating capability towards samarium cation. Assuming that binding of amino acids to Sm(III) (as well as for the other lanthanides) is exclusively through the carboxylate groups, this result is not surprising. Histidine is the only amino acid in this series which presents the possibility to be protonated twice on amino groups (see Table 2). The deprotonated form of the carboxylic acid function exists over a wider pH interval, expanding its coordination capability. Fig. 3 shows the distribution species diagram of this system and the variation of samarium complexation vs. pH under the same conditions.

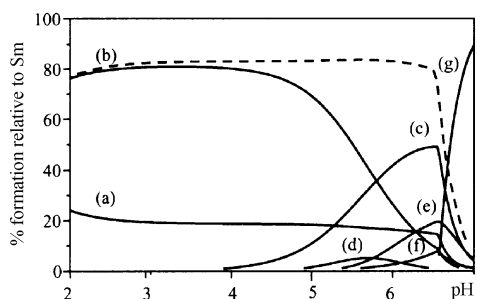


Fig. 3 Species distribution diagram (37.0 °C, 0.15 M NaClO_4) for the Sm–His system. Ligand : metal ratio 3 : 1 and $C_M = 3.0 \text{ mM}$. Thick lines: % formation of (a) Sm^{3+} , (b) $[\text{Sm}(\text{H}_2\text{L})]^{4+}$, (c) $[\text{Sm}(\text{HL})]^{3+}$, (d) $[\text{Sm}_2(\text{HL})_2(\text{H}_2\text{L})_2]^{8+}$, (e) $[\text{Sm}(\text{HL})_3]$, (f) $[\text{Sm}(\text{OH})]^{2+}$, (g) $\text{Sm}(\text{OH})_3 (\text{s})$. Broken line: % complexed Sm vs. pH under the same conditions.

For the Sm(III)– β -Ala system, the most important species present in solution is again $[\text{Sm}(\text{HL})]^{3+}$. Its formation is evident above pH 3.5. Below this pH, the carboxylic group of β -Ala is protonated, preventing coordination. More than 40% of samarium (for $[\text{Sm}^{3+}] = 3 \text{ mM}$, $[\beta\text{-Ala}] = 9 \text{ mM}$) is present as this complex species from pH 4.3 to 6.3. Then, $[\text{Sm}(\text{HL})(\text{OH})_2]^+$ is formed. The latter has a small formation constant, so it appears only in small amounts when the pH is raised and before the precipitation of $\text{Sm}(\text{OH})_3 (\text{s})$ at pH 6.3. Also for this amino acid, a low percentage of samarium (2%) is complexed at pH 7 (for $[\text{Sm}^{3+}] = 3 \text{ mM}$, $[\beta\text{-Ala}] = 9 \text{ mM}$), because the formation of $[\text{Sm}(\text{OH})]^{2+}$ and then $\text{Sm}(\text{OH})_3 (\text{s})$ are more favorable. The capability of β -Ala to stabilize Sm(III) is comparable to α -Ala.⁵ This is in line with the idea that the carboxylate group is the only relevant binding site for coordination.

The isolation of these compounds is a very difficult task due to their high water solubility. In addition, the characterization of the solids is not always easy, taking into account the variable coordination number of the lanthanides and the possibility to incorporate H_2O either in the coordination sphere or in the crystal lattice. However, a few Sm(III)–amino acid complexes have been isolated and studied by X-ray diffraction^{5,27–29} and revealed to be dimeric or polymeric. The amino acid coordinates exclusively through the carboxylate group. Polymerization with carboxylate groups acting as bridges is observed.

For **1**, elemental analysis and TGA results support the formula $[\text{Sm}_2(\text{Pro})_6(\text{H}_2\text{O})_6](\text{ClO}_4)_6$. This complex shows a remarkable difference between the two CO_2 stretching vibrations (symmetric and asymmetric), almost 200 cm^{-1} apart. The shift is close to that of the zwitterionic value, indicating that carboxylate groups are bridging the metals.³⁰

The structure of $[\text{Sm}_2(\text{Pro})_6(\text{H}_2\text{O})_6](\text{ClO}_4)_6$ was solved by X-Ray diffraction analysis. The corresponding ZORTEP diagram is depicted in Fig. 4. Relevant data for the structure

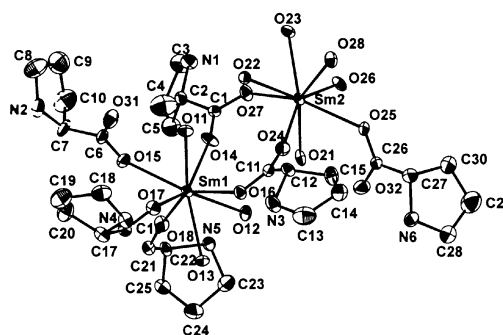


Fig. 4 ZORTEP view of the binuclear cationic complex $[\text{Sm}_2(\text{Pro})_6(\text{H}_2\text{O})_6]^{6+}$ (with labelling scheme). Ellipsoids are drawn with a probability of 30% and the H atoms are excluded for clarity.

are presented in Table 4. The crystal structure of **1** consists of one dimeric unit per unit cell. Each unit has two carboxylate bridges between two samarium atoms. Infinite chains propagated along the (001) direction are formed as shown in Fig. 5. The metal centers are joined by two carboxylate bridges with

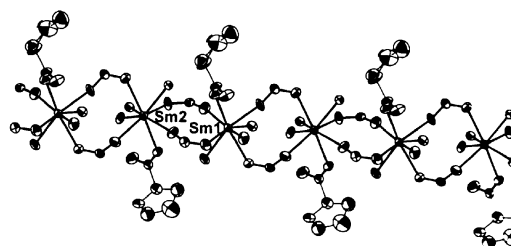


Fig. 5 ZORTEP view of **1** showing the formation of infinite linear chains of proline-bridged Sm atoms. The bridges are shown only with the O–C–O group of atoms.

Table 4 Relevant bond lengths (Å) and angles (°) for **1**

Sm1–O11	2.554(9)	Sm2–O21	2.448(11)
Sm1–O12	2.542(10)	Sm2–O22	2.448(11)
Sm1–O13	2.482(10)	Sm2–O23	2.452(10)
Sm1–O14	2.346(9)	Sm2–O24	2.323(11)
Sm1–O15	2.463(11)	Sm2–O25	2.528(10)
Sm1–O16	2.423(10)	Sm2–O26	2.360(10)
Sm1–O17	2.415(10)	Sm2–O27	2.430(10)
Sm1–O18	2.326(10)	Sm2–O28	2.386(10)
C1–O14	1.252(16)	C1–O27	1.266(16)
C11–O16	1.251(16)	C11–O24	1.222(16)
C6–O15	1.270(17)	C26–O25	1.267(15)
C6–O31	1.206(16)	C26–O32	1.236(15)
O12–Sm1–O11	124.4(4)	O24–Sm2–O22	71.1(4)
O13–Sm1–O11	131.9(4)	O26–Sm2–O22	145.4(4)
O15–Sm1–O11	72.9(4)	O28–Sm2–O22	78.6(3)
O16–Sm1–O11	69.5(4)	O27–Sm2–O22	76.4(4)
O17–Sm1–O11	72.0(3)	O24–Sm2–O21	76.0(4)
O14–Sm1–O11	73.4(4)	O26–Sm2–O21	74.7(3)
O18–Sm1–O11	147.3(4)	O28–Sm2–O21	147.8(4)
O13–Sm1–O12	69.8(4)	O27–Sm2–O21	73.5(4)
O15–Sm1–O12	139.9(4)	O22–Sm2–O21	125.6(3)
O16–Sm1–O12	75.0(4)	O24–Sm2–O23	143.8(4)
O17–Sm1–O12	139.7(4)	O26–Sm2–O23	73.0(4)
O14–Sm1–O12	70.2(4)	O28–Sm2–O23	70.5(4)
O18–Sm1–O12	74.9(4)	O27–Sm2–O23	69.9(4)
O15–Sm1–O13	129.0(4)	O22–Sm2–O23	73.3(4)
O16–Sm1–O13	72.3(4)	O21–Sm2–O23	132.4(4)
O17–Sm1–O13	73.1(4)	O23–Sm2–O25	125.0(3)
O14–Sm1–O13	140.0(4)	O21–Sm2–O25	76.2(3)
O18–Sm1–O13	77.2(4)	O22–Sm2–O25	134.0(3)
O16–Sm1–O15	140.3(4)	O27–Sm2–O25	146.7(4)
O17–Sm1–O15	77.5(4)	O28–Sm2–O25	71.6(4)
O14–Sm1–O15	84.0(5)	O26–Sm2–O25	73.7(4)
O18–Sm1–O15	76.4(4)	O24–Sm2–O25	78.1(4)
O17–Sm1–O16	79.1(4)	O24–Sm2–O26	143.2(4)
O14–Sm1–O16	97.1(4)	O28–Sm2–O27	137.7(4)
O18–Sm1–O16	142.8(4)	O26–Sm2–O27	85.2(4)
O14–Sm1–O17	144.2(4)	O24–Sm2–O27	107.1(4)
O18–Sm1–O17	111.9(4)	O26–Sm2–O28	96.9(3)
O18–Sm1–O14	92.7(4)	O24–Sm2–O28	96.2(4)

Sm–Sm distances of 4.962 and 5.040 Å. These Sm–Sm distances are not identical along the chain because the presence of coordinated water molecules increases the distance. Between two samarium atoms of the dimeric unit, the Sm–Sm distance is 4.962 Å. On the other hand, between two samarium atoms of vicinal dimeric units, four coordinated water molecules cause the Sm–Sm distance to increase to 5.040 Å. The coordination sphere of each samarium atom is completed by one proline acting as a monodentate ligand (also bonded by the oxygen atom of the carboxylate group) and three water molecules. So, the samarium environment consists of five oxygen atoms from five proline carboxylate groups and three water molecules which complete their coordination sphere resulting in a cubic antiprism geometry. The C–O distances (average 1.25 Å) and the O–C–O angle (average 125.2°) clearly show that the carboxyl groups are ionized.

The packing is determined by a network of intermolecular hydrogen bonds involving carboxylic oxygen atoms, perchlorate anions and amine groups. Although no hydrogen water atoms were located, the distances between oxygen atoms in the surrounding water molecules and other groups (amines, oxygen atoms belonging to perchlorate anions and other water molecules) suggest the existence of hydrogen bonds.

It is interesting to compare this structure with those for other lanthanide(III)–proline complexes. [Nd(Pro)₃(H₂O)₂](ClO₄)₃ shows linear polymers in which metallic atoms are connected by two and four carboxylate groups.³¹ Ho and Dy form complexes of general formula [Ln(Pro)₂(H₂O)₅]Cl₃. Once again, a chain can be found, but lanthanides are bridged by a single bidentate proline molecule. Another proline is bonded by only one carboxylate oxygen.³² The last reported structure is that for Er,³³

Table 5 Relevant bond lengths (Å) and angles (°) for **2**

Sm1–O1	2.458(4)	Sm1–O5'	2.388(4)
Sm1–O2	2.428(7)	Sm1–O6	2.444(3)
Sm1–O3	2.392(4)	Sm1–O7''	2.392(4)
Sm1–O4	2.460(4)	Sm1–O8'''	2.357(4)
C1–O5	1.265(7)	C4–O7	1.271(7)
C1–O6	1.242(8)	C4–O8	1.260(7)
O8'''–Sm1–O5''	88.31(16)	O6–Sm1–O1	135.81(13)
O8'''–Sm1–O7''	89.65(16)	O8'''–Sm1–O4	141.23(15)
O5''–Sm1–O7''	149.64(15)	O5''–Sm1–O4	82.29(17)
O8'''–Sm1–O2	98.1(3)	O7''–Sm1–O4	80.49(17)
O5''–Sm1–O2	139.8(2)	O2–Sm1–O4	113.2(3)
O7''–Sm1–O2	70.5(2)	O6–Sm1–O4	71.49(14)
O8'''–Sm1–O6	144.10(17)	O1–Sm1–O4	67.69(15)
O5''–Sm1–O6	81.7(2)	O8'''–Sm1–O3	74.0(2)
O7''–Sm1–O6	115.7(2)	O5''–Sm1–O3	71.6(2)
O2–Sm1–O6	69.9(3)	O7''–Sm1–O3	136.4(2)
O8'''–Sm1–O1	73.55(15)	O2–Sm1–O3	72.21(19)
O5''–Sm1–O1	76.85(19)	O6–Sm1–O3	70.1(2)
O7''–Sm1–O1	73.5(2)	O1–Sm1–O3	134.8(2)
O2–Sm1–O1	143.1(3)	O4–Sm1–O3	135.9(2)
O5–C1–O6	125.0(6)	O7–C4–O8	123.1(5)

Symmetry transformations used to generate equivalent atoms: ' $x, y, z + 1$; '' $2 - x, 0.5 + y, -z$; ''' $2 - x, -0.5 + y, -z$.

with formula [Er(Pro)₂(H₂O)₅]Cl₃. The structure is similar to those of Dy and Ho with one proline acting as a bidentate bridging ligand and another one acting as a monodentate ligand. One-dimensional chains are formed by carboxylate groups bridging two lanthanide ions. The spatial arrangement of **1** is different. There is a double proline bridge and an additional monodentate proline ligand.

For **2**, there is also a complete agreement of analytical results with the proposed formula [Sm(Asp)(H₂O)₄]Cl₂. The structure was also solved by X-ray diffraction analysis. The ZORTEP diagram of [Sm(Asp)(H₂O)₄]Cl₂ is shown in Fig. 6. Relevant

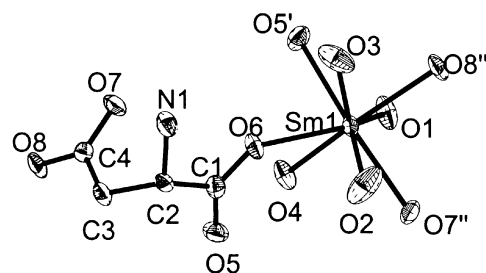


Fig. 6 ZORTEP view of the cation [Sm(Asp)(H₂O)₄]²⁺ (with labelling scheme). Ellipsoids are drawn with a probability of 30% and the H atoms are excluded for clarity.

data for this structure are presented in Table 5. In this structure, the Sm cation is eight coordinated in a distorted bicapped trigonal prism geometry (capped on the quadrilateral faces by oxygen atoms of water molecules). The coordination sphere consists of four water molecules and four aspartic acid residues, two α -CO₂⁻ groups (corresponding to O5' and O6) and two β -CO₂⁻ groups (O7'' and O8'''). A view of the structure along the *a* axis (Fig. 7) shows that the CO₂⁻ groups always act as bridges between Sm atoms. Eleven membered rings are formed, including two Sm atoms at a distance longer than 10 Å. As in the case of **1**, C–O distances show ionized carboxylate groups.

The stoichiometry of the complex includes the presence of a partially ionized amino acid. In the case of glutamic and aspartic acid, complexes with partially deprotonated ligands were isolated and characterized. For glutamic acid, {[Pr₂(Glu)₂(H₂O)₇](ClO₄)₃·11H₂O} and {[Er₂(Glu)₂(NO₃)₂(H₂O)₄](NO₃)₂·5H₂O} were previously characterized.^{34,35} For aspartic acid, {[Ho(Asp)(H₂O)₅]Cl₂·H₂O}_{*n*}, had been previously

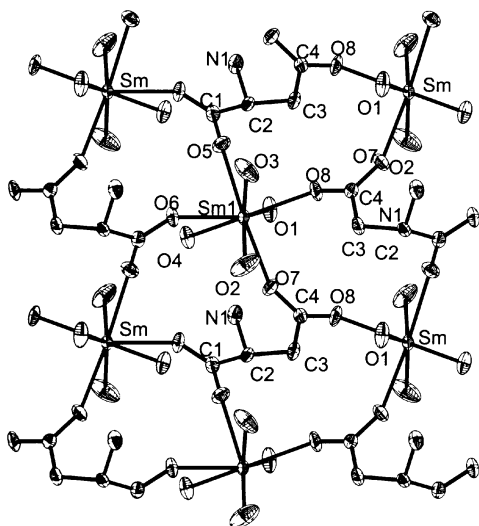
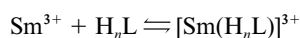


Fig. 7 ZORTEP view of **2** along *a* axis, showing the formation of infinite planes.

reported.³⁶ The structure of **2** is not isostructural with that of Ho. The main difference is the full utilization of CO₂⁻ groups of the amino acid in the coordination.

Concluding remarks

The analysis of potentiometric experimental data for Sm(III)–amino acid systems shows a clear predominance of the monomeric species [Sm(H_{*n*}L)]³⁺, in which the amino acid is in its zwitterionic form. Species containing two or three amino acids per samarium atom in the coordination sphere can be detected, but 1 : 1 species are always predominant. 2 : 1 and 3 : 1 species are formed at pH values near Sm(OH)₃ precipitation, so, they are very difficult to detect. Histidine also forms an [Sm₂(HL)₂(H₂L)₂]⁸⁺ complex. Samarium dimeric complexes with alanine and glycine, [Sm₂(Ala)₄]⁶⁺ and [Sm₂(Gly)₆]⁶⁺ were previously reported and isolated.^{5,29} Depending on pH, species can undergo deprotonation; stability constants for the equilibria:



are in all cases very low and practically independent of the particular amino acid. The logarithm of these formation constants are: 2.37(2) for Ser, 1.03(4) for Arg, 2.87(3) for His, 2.72(4) for Phe, 2.13(7) for Asp and 2.01(3) for β-Ala.

So, coordination of amino acids with Sm(III) is based on very weak interactions between carboxylate groups and the metal ion. This is a consequence of the ionic bond which governs the lanthanide coordination chemistry. The presence of functional groups which increase the acidity of the carboxylic acid is very important in order to obtain complexes which exist over a wide pH interval. This is the case for histidine which shows the greatest ability to retain samarium in solution. Despite the low formation constants, in some Sm–amino acids systems a high percentage of complexation can be detected up to pH 6, due to the existence of deprotonated complexes.

When these systems are studied in solution, monomeric complexes predominate. In the solid state, however, polymeric structures are found. This fact is also very characteristic of complexes of other lanthanides with amino acids.

According to the solid state structures, the carboxylate group seems to be the single binding point of the ligands. If the amino acid possesses more than one acidic group, the additional carboxylate is used to join metallic centers, resulting in polynuclear Sm complexes.

From a radiopharmaceutical point of view, single Sm(III)–amino acid complexes would not be stable enough to reach tumor cells. Even when higher amino acid to samarium molar ratios can be used to prepare the complexes and prevent Sm(OH)₃ (s) formation, the labile character of the lanthanides seems to be a serious problem. For future work, an alternative would be to use stable cores (for example [Sm(EDTA)]⁻) which possess a coordinated and labile H₂O molecule. This water molecule could be substituted by amino acids, resulting in stable complexes. For the design of these new kinds of complex, the better coordination capability of histidine towards Sm(III) should be taken into account. This work is now in progress by our group.

Acknowledgements

The authors gratefully thank PEDECIBA–Química and CONICYT (Uruguayan Organizations) for financial aid and the Spanish Research Council (CSIC) for providing us with a free-of-charge license to the CSD system. Financial support from the Ministerio de Educación, Cultura y Deporte, Spain (Project 9M98-0148) and Programa de Cooperación Científica con Iberoamérica (Uruguay), Project “Nuevos complejos de Samario con aminoácidos y péptidos sencillos de posible uso en Radioterapia” is also acknowledged.

References

- W. A. Volkert and T. J. Hoffman, *Chem. Rev.*, 1999, **99**, 2269.
- M. J. Abrams and B. A. Murrer, *Science*, 1993, **261**, 725.
- S. Jurisson, D. Berning, W. Jia and D. Ma, *Chem. Rev.*, 1993, **93**, 1137.
- J. C. Lattimer, L. A. Corwin, J. Stapleton, W. A. Volkert, G. J. Ehrhardt, A. R. Ketring, J. E. Hewett, J. Simon and W. F. Goeckeler, *J. Nucl. Med.*, 1990, **31**, 586.
- J. Torres, C. Kremer, E. Kremer, H. Pardo, L. Suescun, A. Mombrú, S. Domínguez and A. Mederos, *J. Alloys Compd.*, 2001, **323**, 119.
- J. Torres, C. Kremer, E. Kremer, S. Domínguez, A. Mederos and E. Königsberger, in *Metal Ions in Biology and Medicine*, vol. 6, ed. J. A. Centeno, Ph. Collery, G. Vernet, R. B. Finkelman, H. Gibb and J. C. Etienne, John Libbey Eurotext, Montrouge, France, 2000, p. 774.
- L. G. Sillén, *Ark. Kemi.*, 1953, **5**, 425.
- A. Liberti and I. S. Light, *J. Chem. Educ.*, 1962, **39**, 236.
- P. Gans, A. Sabatini and A. Vacca, *Talanta*, 1996, **43**, 1739.
- L. Alderighi, P. Gans, A. Ienco, D. Peters, A. Sabatini and A. Vacca, *Coord. Chem. Rev.*, 1999, **184**, 311.
- Molecular Structure Corporation, MSC/AFC Diffractometer Control Software, version 5.1.0 MSC, 1993, 3200 Research Forest Drive, The Woodlands, TX 77381, USA.
- G. M. Sheldrick, *Acta Crystallogr., Sect. A*, 1990, **46**, 467.
- G. M. Sheldrick, SHELX97, Programs for Structure Solution and Refinement, University of Göttingen, Germany, 1997.
- A. L. Spek, PLATON. Program for the Automated Analysis of Molecular Geometry, University of Utrecht, The Netherlands, 1990.
- L. Zsolnai and H. Pritzkow, ZORTEP, An Interactive ORTEP Program, University of Heidelberg, Germany, 1995.
- M. Nair, E. Chellam, P. T. Arasu and C. Natarajan, *Indian J. Chem.*, 1990, **29A**, 1233.
- G. Berthon and P. Germonneau, *Agents Actions*, 1982, **12**, 619.
- M. Maeda, M. Tsunoda and Y. Kynjo, *J. Inorg. Biochem.*, 1992, **48**, 227.
- M. Maeda, K. Okada, Y. Tsukamoto and K. Wakabayashi, *J. Chem. Soc., Dalton Trans.*, 1990, 2337.
- M. Nair, M. Santappa and P. Natarajan, *Indian J. Chem.*, 1980, **8**, 1312.
- A. Corrie, G. Makar and D. Williams, *J. Chem. Soc., Dalton Trans.*, 1975, 105.
- A. Corrie, G. Makar and D. Williams, *J. Chem. Soc., Dalton Trans.*, 1976, 1068.
- S. N. Limaye and M. C. Saxena, *Can. J. Chem.*, 1986, **64**, 865.
- P. R. Reddy and V. B. M. Rao, *Inorg. Chim. Acta*, 1986, **125**, 191.
- S. Zielinski, L. Lomozik and A. Wojciechowska, *Monatsh. Chem.*, 1981, **112**, 1245.
- H. G. Brittain, *Inorg. Chem.*, 1979, **18**, 1740.

- 27 R. Wang, Z. Zheng, T. Jin and R. J. Staples, *Angew. Chem., Int. Ed.*, 1999, **38**, 1813.
- 28 A. Ma, L. Li, Y. Lin, S. Jin and S. Xi, *Chin. J. Appl. Chem.*, 1993, **10**, 110.
- 29 A. Ma, L. Li, Y. Lin and S. Xi, *Wuji Huaxue Xuebao (J. Inorg. Chem.)*, 1993, **9**, 401.
- 30 K. Nakamoto, *Infrared and Raman Spectra of Inorganic and Coordination Compounds*, 5th edn., Wiley, New York, 1997.
- 31 J. Legendziewicz, T. Glowiak, E. Huskowska and C. N. Dao, *Polyhedron*, 1988, **7**, 2495.
- 32 J. Legendziewicz, T. Glowiak, E. Huskowska and C. N. Dao, *Polyhedron*, 1989, **8**, 2139.
- 33 A. Z. Ma, L. M. Li, Y. H. Lin and S. Q. Xi, *Acta Crystallogr., Sect. C*, 1993, **49**, 865.
- 34 Q. Jin, X. Wang, T. Jin, G. Xu and S. Zhang, *Polyhedron*, 1994, **13**, 2957.
- 35 I. Csöreg, P. Kierkegaard, J. Legendziewicz and E. Huskowska, *Acta Chem. Scand., Ser. A*, 1987, **41**, 453.
- 36 I. Csöreg, P. Kierkegaard, J. Legendziewicz and E. Huskowska, *Acta Chem. Scand.*, 1989, **43**, 636.